Research Square

Preprints are preliminary reports that have not undergone peer review.
They should not be considered conclusive, used to inform clinical practice,
or referenced by the media as validated information.

Integrative analysis of organellar genomes and transcriptomes reveals key organelle-nuclear crosstalk modules in Paliurus hemsleyanus

Botao Ye
Luoyang Normal University
Rong Chen
Chinese Academy of Sciences
Xuhui Li
Shenzhen University
Shiting Yang
Chinese Academy of Sciences
Haoxing Li
Chinese Academy of Sciences
Yanzhao Zhang
yzhao_zhang@163.com

Luoyang Normal University

Research Article

Keywords: Paliurus hemsleyanus, mitochondrial genome, chloroplast genome, nuclear-organelle interaction, phylogenetic analysis, Rhamnaceae

Posted Date: September 8th, 2026

DOI: https://doi.org/10.21203/rs.3.rs-10464236/v1

License: This work is licensed under a Creative Commons Attribution 4.0 International License.
Read Full License

Additional Declarations: No competing interests reported.

Abstract

Paliurus hemsleyanus Rehd. is recognized for its robustness, economic value, and ornamental appeal, and it is commonly employed as a rootstock for *Ziziphus jujuba* Mill.. Although this species holds ecological and economic importance, the organelle genome resources and the interplay networks between nuclear and organellar genes in this species are still scarce. This work presents the first high-quality assembly and systematic comparative analysis of the mitochondrial and chloroplast genomes of *P. hemsleyanus*. Organelle genomic features were comprehensively investigated, covering genomic organization, gene composition, codon preference, repeat elements, RNA editing modification, MTPT transfer events, collinearity relationships, phylogenetic relationships, and adaptive selection pressure (Ka/Ks ratios). In addition to structural genomic analysis, transcriptome datasets derived from roots, stems and leaves were further integrated to dissect the protein-protein interaction network between nuclear and organellar components in *P. hemsleyanus*. Some hub genes were finally screened out, which serve as vital regulators to modulate the molecular crosstalk between nuclear-derived and organelle-coding genes. This high-quality organellar genome clarifies the evolutionary trajectory of *P. hemsleyanus* and identifies core molecular targets for leaf development improvement in future breeding. It also establishes a novel framework for exploring organellar-nuclear co-evolution in Rhamnaceae, and offers fundamental genetic resources for evolutionary analysis, functional genomics, molecular breeding and germplasm conservation of Rhamnaceous species.

1. Introduction

As a member of the widespread genus *Paliurus* of Rhamnaceae, *Paliurus hemsleyanus* Rehd. is a valuable deciduous shrub or small tree, which is conventionally called Chinese Coin Tree [1]. Endemic to the mountainous forests of China, it exhibits strong adaptability to diverse environments. Cointree offers notable economic value due to bioactive triterpenoids in its roots, while also providing key ecological functions such as soil conservation and slope stabilization [1, 2]. Importantly, it acts as an ideal rootstock for *Ziziphus jujuba* Mill., one of China's most economically important forest species. Grafting cointree scions onto jujube rootstock significantly improves tolerance to jujube witches' broom disease, the most destructive pathogen limiting jujube cultivation worldwide [3, 4]. Despite its ecological and economic importance, the cointree currently lacks comprehensive genomic resources, including chloroplast and mitochondrial genomes, nuclear-encoded genes, and organelle protein–protein interaction (PPI) data. This deficiency underscores the urgent need for a high-quality genome assembly to better understand its genomic architecture and evolutionary history.

Eukaryotic mitochondria and chloroplasts evolved from ancient endosymbiosis, an evolutionary viewpoint that has been well documented in previous studies [5]. Both organelles retain autonomous genetic systems separate from the nuclear genome, while closely cooperating with nuclear components to sustain normal physiological functions [6]. Plant mitochondrial genomes generally show larger size and higher structural complexity, with an extremely variable length ranging from 100 to 10,000 kb, diverse organizational architectures, sparse gene distribution, and abundant repetitive fragments [7, 8].

These inherent properties greatly hinder the accurate assembly and structural characterization of plant mitogenomes [9]. On the contrary, angiosperm chloroplast genomes maintain a highly compact and simple configuration, encoding roughly 120–130 functional genes with a moderate genome size of 107–218 kb [10] .

Despite their essential roles in plant growth and development, mitochondrial genomes remain far less studied than chloroplast genomes. As of early 2026, NCBI data show only 633 complete plant mitogenomes deposited, compared with 9,993 chloroplast genomes—a disparity largely driven by the structural complexity of mitochondrial DNA [8]. Extreme size variation exemplifies their evolutionary divergence: the largest known plant mitogenome belongs to Silene conica (11.3 Mb), while the smallest is from *Viscum scurruloideum* (66 kb) [7]. This high variability contrasts sharply with the structural conservation of plastid genomes, reflecting distinct evolutionary trajectories for the two organellar genomes. Although high-quality nuclear reference genomes of *P. hemsleyanus* are already available, assembly analysis of the *P. hemsleyanus* mtGenome and cpGenomes has not been comprehensively and systematically reported. Multi-omics combined analysis establishes a solid research framework to dissect the regulatory networks and potential molecular mechanisms that govern complex agronomic and biological traits [11].

In the present study, we report a comprehensive investigation and comparative assessment of the complete mitochondrial genomes and chloroplast genomes of *P. hemsleyanus*. This thorough evaluation facilitated our exploration of multiple key characteristics of *P. hemsleyanus*, including structural organization, gene content, codon usage preference, repetitive sequence profiles, RNA editing sites, mitochondrial-plastid DNA transfer (MTPT) events, syntenic conservation, phylogenomic positioning, and selection pressure as evaluated using the ratio of non-synonymous to synonymous substitutions (Ka/Ks). Notably, we incorporated transcriptome data from roots, stems, and leaves of *P. hemsleyanus* to analyze differentially expressed nuclear genes that target mitochondrion and chloroplast. For *P. hemsleyanus*, we further constructed comprehensive nuclear-organelle protein-protein interaction (PPI) networks by integrating nuclear-encoded, organelle-targeted proteins with organelle-encoded proteins directly derived from the chloroplast and mitochondrial genomes. Through this integrative network analysis, some genes were identified as core candidate genes in the nuclear-chloroplast and nuclear-mitochondrial PPI networks, respectively. This study is expected to substantially expand the available organelle genome resources within the Rhamnaceae family and lay a critical foundation for the classification and molecular breeding of *P. hemsleyanus*. Furthermore, this research aims to provide novel perspectives on the organelle-nuclear crosstalk that underlies the evolution of *P. hemsleyanus* and identify a primary target for future molecular breeding initiatives.

2. Materials and methods

2.1 Data acquisition, assembly and annotation of the *P. hemsleyanus* mitogenomes

To construct the mitochondrial genome and chloroplast genome of *Paliurus hemsleyanus*, we downloaded PacBio sequencing data for *Paliurus hemsleyanus* from the Genome Sequence Archive database (CRR1721099) (https://ngdc.cncb.ac.cn/gsa/browse/CRA024427/CRR1721099) [1]. We used Oatk v1.0 software to simultaneously assemble the mitochondrial and plastid genomes from the PacBio HiFi reads [12]. The assembly was conducted using a *k*-mer size of 1001 and a minimum coverage threshold of 30. To facilitate the automated resolution of the organellar genome graphs, default plant-specific HMM profiles were integrated via nhmmscan. The complete mitogenomes and chloroplast genomes of *Paliurus hemsleyanus* were initially annotated using the online tools PMGA [13] and GeSeq [14], respectively. Then, the codons and gene boundaries were checked and manually corrected using Geneious v2022.2.1 [15], with reference to the published mitogenome of *Ziziphus jujuba* (NC_029809) and the chloroplast genome of *Paliurus hemsleyanus* (NC_070046). Finally, high-resolution circular genome maps were visualized using OGDRAW [16] .

2.2 Analysis of codon usage bias and repeat fragments

To characterize the codon usage bias and repetitive landscape of the assembled mitogenome and chloroplast genome of *Paliurus hemsleyanus*, the Relative Synonymous Codon Usage (RSCU) values for both genomes were calculated using the "uco" function from the R package *seqinr* [17].

Three categories of repetitive sequences were detected in the mitogenome and chloroplast of *Paliurus hemsleyanus*, namely Simple Sequence Repeats (SSRs), Tandem Repeats (TRs), and Dispersed Repeats (DRs). SSRs were identified through the MISA web server [18], with the minimum repeat unit thresholds configured as follows: 10 repeats for mononucleotide SSRs, 6 repeats for dinucleotide SSRs, 5 repeats for trinucleotide SSRs, and 4 repeats each for tetra-, penta-, and hexanucleotide SSRs. Simultaneously, tandem repeats (TRs) were analyzed using the Tandem Repeats Finder (TRF) software [19]. The analysis was performed with the default scoring parameters (a match score of 2, a mismatch penalty of 7, and an indel penalty of 7), coupled with a minimum alignment score of 50 to filter out low-confidence tandem repeat loci. Dispersed repetitive sequences, including forward, reverse, palindromic, and complementary repeat types, were identified by means of the Vmatch program [20]. To ensure the reliability of detection, the analysis was conducted with a minimum repeat length of 30 bp and a Hamming distance of 3. Finally, quantitative bar charts were employed to visualize the comparative distribution patterns and density of these three types of repetitive elements, including SSR profiles, TR distribution patterns, and DR content, providing intuitive insights into the repetitive sequence landscape of the *Paliurus hemsleyanus* mitogenome.

2.3 Prediction of RNA editing sites and identification of MTPTs

The identification of C-to-U RNA editing sites within mitochondrial protein-coding genes (PCGs) was performed using Deepred-mt [21]. MTPTs were identified by performing a localized genomic alignment between the *Paliurus hemsleyanus* plastome and mitogenome sequences using BLASTn [22]. The

alignment was executed using the megablast task, with filtering parameters strictly set to an E-value threshold of $1x10^{-5}$ and a minimum sequence identity of 80%.

To ensure precise characterization of horizontal gene transfer occurrences, redundant mitochondrial derived plastid sequences (MTPTs), for instance those located in the inverted repeat (IR) domains of the plastid genome, were counted as single entries only. The recovered MTPT sequences were then functionally annotated with GeSeq software [14], and the positional correlations between the two organellar genomes were graphically displayed using the Circos toolkit [23].

2.4 Phylogenomic characterization and evolutionary analysis of *P. hemsleyanus* mitogenomes

To investigate structural evolutionary features and assess assembly integrity, a comparative synteny analysis was performed between the mitogenomes of *Paliurus hemsleyanus* and three closely related accessions: *Frangula alnus* Mill. (NC_065239), *Ziziphus jujuba* (PP035764), and *Ziziphus mauritiana* Lam. (OP537228). Locally Collinear Blocks (LCBs) were identified through genome alignments using Mauve v2.4.0 [24]. Visualization of multiple synteny plots was executed via the online platform ChiPlot (https://www.chiplot.online/) to highlight genomic rearrangements.

To evaluate selection pressures on PCGs, shared PCGs among the *Paliurus hemsleyanus* mitogenome and three closely related accessions were extracted using Geneious [15]. Subsequently, sequence alignments were performed using MAFFT v7.471 [25, 26]. The KaKs_Calculator 3.0 tool was used to determine the Ka/Ks ratio of each PCG [25, 27].

To determine the taxonomic placement of *Paliurus hemsleyanus*, mitochondrial genome sequences from 21 representative species across the families Elaeagnaceae, Fabaceae, Moraceae, Rhamnaceae, Rosaceae and Gramineae were retrieved from the NCBI GenBank database. A shared set of 27 orthologous PCGs common to all 21 analyzed species was extracted. Individual PCGs were aligned using MAFFT v7.471 [25, 26]. The trimmed alignments of all 27 genes were concatenated into a single supermatrix for subsequent phylogenetic analysis. Phylogenetic inference was performed using the Maximum Likelihood (ML) method in RAxML v8.2.12 with the GTRCAT model. Rapid bootstrap with 1,000 replicates was utilized to compute bootstrap support values (MLBS) for each node of the ML tree [28]. The resulting topology was visualized and decorated using tvBOT [29].

2.5 Transcriptome and differential expression analysis

In the current research, publicly available RNA-seq data of *P. hemsleyanus* roots, stems and leaves were retrieved from the China National Center for Bioinformation (CNCB) under BioProject PRJCA038194 (https://ngdc.cncb.ac.cn/bioproject/browse/PRJCA038194) [1]. Raw transcriptomic reads were processed with fastp software for rigorous quality filtering, which effectively trimmed adapter contaminants and low-quality nucleotide bases [30]. The retained high-quality clean reads were mapped to the reference genome of *P. hemsleyanus* with default parameter settings [31]. After genome alignment, gene transcript reconstruction and expression abundance quantification were completed

using the featureCounts program [32]. Differentially expressed genes (DEGs) across leaf-root and leaf-stem tissue groups were screened with the edgeR package. Gene expression abundance was calculated and standardized with TPM and FPKM normalization methods [33]. In this study, genes with $|\log_2(\text{fold change})| \geq 1$ and Benjamini-Hochberg corrected p-value < 0.05 were regarded as significant DEGs. Furthermore, the clusterProfiler tool was used to carry out Gene Ontology (GO) functional annotation and Kyoto Encyclopedia of Genes and Genomes (KEGG) pathway enrichment analyses, aiming to explore the potential biological functions and metabolic pathways of the identified DEGs [34].

2.6 Subcellular localization and PPI network analysis

To explore the functional characteristics of genes showing significant expression differences across roots, stems, and leaves of *P. hemsleyanus*, we predicted protein subcellular localization using three well-established tools: WoLF PSORT, TargetP 2.0, and DeepLoc [35–37]. This combined approach allows robust and comprehensive assignment of proteins to subcellular compartments based on inherent amino acid sequence properties. We then focused on differentially expressed genes with striking expression shifts that were specifically localized to mitochondrion or chloroplast, and constructed PPI networks to reveal their functional cooperation within organellar contexts. Using *Arabidopsis thaliana* as the reference organism, protein interaction relationships were predicted via the STRING database [38], with organelle-encoded proteins from *P. hemsleyanus* serving as reference sequences. Only high-confidence interaction pairs were retained to ensure network reliability. The final networks were visualized and refined in Cytoscape v3.9 [39], enabling identification of key hub genes and functional modules potentially associated with leaf development.

3. Results

3.1 Genomic characterization of mitochondrial and chloroplast genomes in *P. hemsleyanus*

The complete mitochondrial genome of *P. hemsleyanus* displayed two circular organizations, spanning 389,300 bp in total and possessing an overall GC content of 45% (Fig. 1a). Gene prediction and annotation analyses identified 65 genes in the mitochondrial genome, comprising 37 PCGs, 3 ribosomal RNA genes, and 16 transfer RNA genes. These PCGs were systematically categorized into functional groups, primarily comprising: ATP synthase (Complex V: *atp1*, *atp4*, *atp6*, *atp8*, *atp9*); cytochrome c biogenesis (*ccmb*, *ccmc*, *ccmfc*, *ccmfn*); Ubiquinol cytochrome c reductase (cob); cytochrome c oxidase (Complex IV: *cox1*, *cox2*, *cox3*); RNA maturase (*matR*); Transport membrane protein (*matB*); NADH dehydrogenase (Complex I: *nad1*, *nad2*, *nad3*, *nad4*, *nad4L*, *nad5*, *nad6*, *nad7* and *nad9*); Ribosomal proteins (LSU) (*rpl5*, *rpl10* and *rpl16*); Ribosomal proteins (SSU) (*rps1*,*rps10*, *rps12*, *rps13*, *rps19*, *rps3*, *rps4* and *rps7*); succinate dehydrogenase (Complex II: *sdh3* and *sdh4*) (Table S1).

The chloroplast genome of *P. hemsleyanus* formed a typical circular structure, with a total length of 160,470 bp and an average GC content of 37% (Fig. 1b). The complete chloroplast genome of *P.*

hemsleyanus contained a total of 113 unique annotated genes (excluding redundant copies in the inverted repeat regions), including 79 distinct PCGs, 4 ribosomal RNA genes, and 30 transfer RNA genes. These genes were functionally assigned to four major categories: genes for photosynthesis, genes for self-replication, other functional genes, and genes of unknown function. The photosynthesis-related genes comprised 46 genes encoding subunits of key photosynthetic complexes, including 11 subunits of NADH dehydrogenase, 7 subunits of photosystem I, 15 subunits of photosystem II, 6 subunits of ATP synthase, 6 cytochrome-related subunits, and 1 gene encoding the large subunit of Rubisco. The self-replication-related category included 59 genes responsible for the chloroplast's replication and translation machinery, namely 4 RNA polymerase genes, 12 small subunit ribosomal protein genes, 9 large subunit ribosomal protein genes, 4 ribosomal RNA genes, and 30 transfer RNA genes covering all 20 amino acids. Additionally, 6 genes with diverse functions were identified, including one membrane protein gene (*cemA*), one maturase gene (*matK*), one proteolysis-related gene (*clpP*), one translation initiation factor gene (*infA*), one acetyl-CoA carboxylase gene (*accD*), and one cytochrome c synthesis gene (*ccsA*). Two conserved open reading frames (*ycf1* and *ycf2*) of unknown function were also present. Furthermore, 17 genes in the chloroplast genome contained introns: two genes (*ycf3* and *clpP*) harbored two introns each, while the remaining 14 genes (*ndhA*, *ndhB*, *petB*, *petD*, *rpoC1*, *rps12*, *rps16*, *rpl2*, *rpl16*, *trnA-UGC*, *trnG-UCC*, *trnI-GAU*, *trnK-UUU*, *trnL-UAA*, and *trnV-UAC*) each contained a single intron (Table S2).

3.2 Codon usage bias and RSCU analysis

To investigate the codon usage characteristics of PCGs in the mitochondrial and chloroplast genomes of *P. hemsleyanus*, a comprehensive analysis of codon usage bias was performed on all 37 mitochondrial and 79 chloroplast PCGs, which contained 10,673 and 22,929 codons, respectively, covering 20 amino acids and termination signals (Fig. 2 and Table S3). The most frequently used codon was UUU (Phe, 376 occurrences) in the mitochondrial genome and AUU (Ile, 977 occurrences) in the chloroplast genome. Leucine (Leu) was the most abundant amino acid in both genomes (1,118 in mitochondrion, 2,417 in chloroplast), while termination codons were the least frequent (53 vs 79). RSCU analysis revealed that 30 preferred codons (RSCU > 1.0) were detected in both organelles; of these, 27 (mitochondrion) and 29 (chloroplast) ended in A or U. Correspondingly, 32 non-preferred codons (RSCU < 1.0) were identified in both genomes. The single-copy codons AUG (Met) and UGG (Trp) consistently showed RSCU values of exactly 1.0 in both organelles, indicating no usage bias and high evolutionary conservation. These distinct RSCU patterns reflect organelle-specific mutational pressures and tRNA repertoires, providing insights into the evolutionary forces shaping codon usage in plant organelle genomes.

3.3 Analysis of repeat sequences

Repetitive elements are key drivers of structural plasticity and evolutionary dynamics in plant organellar genomes. In this work, we systematically characterized two major classes of repeats across the mitochondrial and chloroplast genomes of *P. hemsleyanus*.

Screening with the MISA pipeline uncovered 102 SSR loci in the mitochondrial genome, compared to 65 loci in the chloroplast genome (Fig. 3a and Table S4). Mononucleotide repeats dominated both organellar repeat profiles: 86 loci (84.31% of total mitochondrial SSRs) and 63 loci (96.92% of total chloroplast SSRs) fell into this category. Dinucleotide repeats represented the second-largest fraction, with 13 copies (12.75%) in the mitochondrion versus just 1 copy (1.54%) in the chloroplast. Trinucleotide repeats were sparse in both compartments (2 copies, 1.96% in mitochondrion; 1 copy, 1.54% in chloroplast), while tetranucleotide repeats were restricted to the mitochondrial genome (1 copy, 0.98%) and entirely absent from the chloroplast genome.

A stark divergence in dispersed repeat abundance and composition was also observed between the two organelles (Fig. 3b and Table S5). The mitochondrial genome contained 734 dispersed repeats, categorized as 13 tandem, 151 forward, 194 palindromic, and 376 reverse repeats. Reverse repeats constituted the most prevalent class, followed by palindromic repeats. Conversely, the chloroplast genome harbored only 201 dispersed repeats, including 82 tandem, 32 forward, 33 palindromic, and 52 reverse repeats. Complementary repeats were not detected in the mitochondrial genome, while a small set of 2 complementary repeats was identified in the chloroplast genome.

3.4 Prediction of RNA editing sites and characterization of mitochondrial plastid DNA

RNA editing constitutes a vital post-transcriptional regulatory mechanism that ensures functional gene expression in plant mitochondria. In this study, we systematically predicted RNA editing sites across all PCGs in the *P. hemsleyanus* mitochondrial genome. A total of 49 editing sites were identified in the *nad4* gene, representing the highest count among all genes analyzed (Fig. 4a and Table S6). The number of editing sites varied substantially across genes, with *ccmB* (35 sites), *nad7* (36 sites), *matR* (33 sites), and *nad1* (33 sites) also exhibiting high editing frequencies. In contrast, several genes, including *rps7* and *sdh4*, harbored only 2–7 editing sites, indicating a broad range of editing events across different mitochondrial transcripts.

Inter-organellar DNA transfer is a prominent feature of plant organellar genome evolution. To investigate the MTPTs in *P. hemsleyanus*, a detailed analysis of homologous segments between the mitochondrial and chloroplast genomes was performed. A total of 17 MTPT fragments were identified, with a cumulative length of 17,718 bp, accounting for approximately 4.55% of the total 389,300 bp mitogenome size. The lengths of these MTPT fragments ranged from 31 bp to 7,219 bp, with 14 fragments distributed on mtDNA chr1 and 3 fragments on mtDNA chr2 (Fig. 4b and Table S7). The circular alignment map further revealed extensive sequence homology between the circular mitochondrial genome and the 160,470 bp circular chloroplast genome: colored arcs within the plot represent regions of sequence similarity, and the distribution of these homologous segments was non-uniform across the mitochondrial genome, with 12 fragments located in intergenic regions and 5 fragments overlapping with conserved tRNA genes.

Annotation of these MTPT fragments revealed that all transferred plastid genes were tRNA genes, with a total of 4 distinct conserved tRNA loci identified, including *trnM-CAU*, *trnN-GUU*, *trnD-GUC*, and *trnH-GUG* that were present in both organellar genomes. No plastid-derived PCGs or rRNA genes were detected in the *P. hemsleyanus* mitochondrial genome. These findings suggest that tRNA gene transfer events from the chloroplast to the mitochondrion have occurred during the evolutionary history of the *P. hemsleyanus* mitochondrial genome, reflecting the dynamic nature of inter-organellar DNA transfer and the contribution of chloroplast sequences to the structural and evolutionary complexity of the mitogenome.

3.5 Synteny analysis, evolutionary rates and phylogenetic placement

To investigate the structural evolution of the *P. hemsleyanus* mitochondrial genome and assess its assembly quality, a comparative collinearity analysis was conducted with three closely related Rhamnaceae species: *Frangula alnus*, *Ziziphus jujuba*, and *Ziziphus mauritiana*. The analysis revealed extensive sequence homology across the four genomes, with shared syntenic blocks linked by red lines (Fig. 5a). Despite the high degree of homology, the collinearity plot highlights widespread structural rearrangements, indicating frequent genomic reshuffling events during the evolution of Rhamnaceae mitochondrial genomes.

To explore the evolutionary pressures acting on mitochondrial PCGs, the ratio of Ka/Ks was calculated (Fig. 5b and Table S8). Most genes showed Ka/Ks values below 1, indicating strong purifying selection. However, several genes displayed signals of relaxed or positive selection. The *atp8* gene exhibited the highest Ka/Ks ratio (> 2), suggesting strong positive selection. Other genes such as *ccmFc*, *matR*, *nad1*, *rpl5* and *rps4* also showed elevated Ka/Ks values (above 1), consistent with positive or relaxed selective pressure. In contrast, genes involved in core respiratory functions (e.g., *atp1*, *atp4*, *cox1*, *cox2*) generally displayed Ka/Ks values below 0.5, indicating strong purifying selection to maintain functional integrity.

To resolve the phylogenetic position of *P. hemsleyanus*, a ML tree was constructed using concatenated core mitochondrial PCGs from 21 representative species across 6 families (Fig. 5c and Table S9). The phylogenetic tree strongly supports the monophyly of the Rhamnaceae family, with *P. hemsleyanus* forming a well-supported clade with *Frangula alnus*, *Ziziphus jujuba*, and *Ziziphus mauritiana*. All species clustered into their respective families with high bootstrap support, including Moraceae, Elaeagnaceae, Rosaceae, Fabaceae, and Gramineae, consistent with established taxonomic relationships.

3.6 Transcriptome expression profiling and functional annotation

To characterize transcriptional divergence across different vegetative tissues of *P. hemsleyanus*, we performed a comparative transcriptomic analysis of roots, stems, and leaves, identifying tissue-specific patterns of gene expression and functional enrichment.

GO enrichment analysis revealed distinct functional profiles for DEGs in root-leaf and stem-leaf comparisons (Fig. 6a, 6b). In both contrasts, the most significantly enriched biological process (BP) terms were strongly associated with photosynthesis and plastid function, including photosynthesis; photosynthesis, light harvesting; photosynthesis, light reaction; plastid organization; chloroplast organization, and generation of precursor metabolites and energy. Consistently, cellular component (CC) categories were dominated by terms related to photosynthetic structures, such as thylakoid, plastid thylakoid, chloroplast thylakoid, and photosynthetic membrane. At the molecular function (MF) level, the root-leaf comparison showed enrichment in monooxygenase activity and microtubule motor activity, while the stem-leaf contrast was characterized by UDP-glycosyltransferase activity, beta-glucosyltransferase activity, and tetrapyrrole binding. These patterns reflect the fundamental divergence in photosynthetic and metabolic functions between non-photosynthetic (root and stem) and photosynthetic (leaf) tissues.

Complementary KEGG pathway enrichment further highlighted tissue-specific metabolic reprogramming (Fig. 6c, 6d). For root-leaf DEGs, the most prominent pathways included glycolysis, glutathione metabolism, porphyrin metabolism, and carbon fixation in photosynthetic organisms. The stem-leaf contrast revealed enrichment in phenylpropanoid biosynthesis, biosynthesis of various plant secondary metabolites, starch and sucrose metabolism, and flavonoid biosynthesis. These differences underscore the specialized metabolic roles of each tissue: roots are associated with primary metabolism and stress responses (glutathione and glycolysis), stems with secondary metabolism and carbohydrate partitioning, and leaves with photosynthesis and carbon fixation.

3.7 PPI network of differentially expressed nuclear-encoded genes and mitochondrial genes

To pinpoint the critical regulatory factors that mediate PPI networks between the nucleus and organelles, we carried out an exhaustive subcellular localization analysis of the identified DEGs. Employing a consensus strategy across three independent bioinformatic tools (TargetP, WoLF PSORT, and DeepLoc), we selected 72 candidate genes—50 targeted to chloroplast and 22 targeted to mitochondrion—that were consistently predicted to localize to their respective organelles by all three platforms. These high-confidence organelle-targeted candidates were then used to construct PPI networks linking nuclear genes to organellar gene products (Table S10). Building on this set of reliable candidates, we further analyzed and deciphered the molecular interaction patterns associated with chloroplast and mitochondrial functions in a separate manner.

To dissect the molecular interactions underlying photosynthesis and chloroplast function, we analyzed the PPI network formed by nuclear DEGs and chloroplast-encoded proteins (Fig. 7a), whose core is dominated by essential photosynthetic and carbon fixation machinery, including subunits of photosystem I/II, the cytochrome b_6f complex, ATP synthase, and chloroplast ribosomal proteins. Key nuclear-encoded hubs in this network include RBCS-1A and RBCS-3B (small subunits of Rubisco) that form a central sub-network with Calvin cycle enzymes such as GAPA1 and FBA2 to link nuclear

expression to carbon fixation efficiency; light-harvesting complex proteins (LHCA1, LHCA2, LHCA3, LHCA4, and LHCB5) that form a highly interconnected module with photosystem core components for light harvesting and energy transfer; chaperonin subunits CPN60A1 and CPN60B1 that facilitate protein folding and photosynthetic complex assembly; FD1 (Ferredoxin 1) that acts as a major hub mediating electron flow and redox regulation through extensive connections to the photosynthetic electron transport chain; and RCA (Rubisco activase) that maintains Rubisco activity and carbon fixation by linking closely to Rubisco subunits. Additional nuclear-encoded proteins including Lhb1B1, TKL-2, THI1, DRT112, PETs, HSP70-6, GLN2, THIC, PORA, CURT1A, RH3, PSBR, and CPN20 are distributed across the network periphery, contributing to chlorophyll biosynthesis, thylakoid organization, and stress responses, collectively illustrating the coordination between nuclear-encoded proteins and chloroplast components in maintaining photosynthetic efficiency, carbon fixation, and chloroplast homeostasis.

To explore the functional relationships between nuclear DEGs and mitochondrial gene products, we constructed the corresponding PPI network (Fig. 7b), whose core is dominated by components of the mitochondrial respiratory chain (e.g., COX1/2/3, NAD4/7/9, ND4L, ATP6-1, MT-CYB, SDH4) and ribosomal proteins (e.g., RPS7/10/12/13/19, RPL16) that form a tightly interconnected module central to energy metabolism and translation. Key nuclear-encoded regulators in this network include T20K12.260, which occupies a distinct position interacting with multiple respiratory chain and ribosomal components to potentially regulate mitochondrial biogenesis or function; PYD4, a peripheral but functionally relevant node linking pyrimidine metabolism to mitochondrial energy processes; SHM1 (Serine hydroxymethyltransferase 1) that connects to core respiratory and ribosomal proteins to participate in one-carbon metabolism and mitochondrial redox balance; GDH2 (Glutamate dehydrogenase 2) and FDH1 (Formate dehydrogenase 1) that associate with the central respiratory network to link amino acid and one-carbon metabolism to mitochondrial energy production; PURU2, NDPK3, and LPD1-2 that integrate into the network to contribute to nucleotide metabolism, energy transfer, and mitochondrial redox regulation; and F24F17.2, a distinct peripheral node potentially involved in mitochondrial stress responses or secondary metabolic regulation. The overall network topology reveals the interface between nuclear-encoded proteins and mitochondrial core machinery, highlighting the coordination between primary metabolism, energy production, and organellar function in *P. hemsleyanus*.

4. Discussion

4.1. Characterization, codon usage bias and repeat sequences of mtGenomes and cpGenomes in *P. hemsleyanus*

Mitochondria and chloroplasts are essential organelles in plants, with mitochondria serving as the primary energy supply hub and chloroplasts mediating photosynthesis and carbon fixation—both playing indispensable roles in plant growth, development, and environmental adaptation [40]. Prior research has identified multiple structural forms of the mitogenome, including circular, linear, branched, and numerous

mini-circle molecules [41]. Chloroplast genomes (cpgenomes), by contrast, typically display a conserved circular quadripartite structure (large single-copy, small single-copy, and two inverted repeats), though variations in size and gene content can occur across species [42]. *P. hemsleyanus* is an economically and ecologically important Rhamnaceae species, yet its organellar genomes have not been fully resolved in detail. In the present study, we comprehensively assembled and characterized the mitogenome and cpgenome of *P. hemsleyanus*, providing novel insights into their structural features and evolutionary dynamics.

With a total length of 389,300 bp and a GC content of 45%, the mitogenome of *P. hemsleyanus* adopts a canonical circular conformation. Its size is larger than that of *Ziziphus mauritiana* Lam., *Ziziphus jujuba*, and *Fragaria species*, yet smaller than that of *Malus domestica*, *Prunus davidiana*, and *Prunus salicina* [43–48] .

Previous studies have shown that mitochondrial gene order and structural architecture remain relatively conserved. Notably, the gene counts in *Malus domestica* (63) and *Prunus davidiana* (64) are considerably higher than those observed in *Prunus salicina* (37), *P. hemsleyanus* (37), *Ziziphus jujuba* (39), *Ziziphus mauritiana* Lam. (34), and *Fragaria* species (30) [43–48]. This size variation is likely attributable to differences in repetitive DNA content and inter-organellar gene transfer, which are known drivers of plant mitogenome expansion [49]. The GC content (45%) falls within the highly conserved range (43–46%) reported for angiosperm mitogenomes [50], indicating strong selective constraints on base composition. The mitogenome encodes 65 genes (37 PCGs), a number comparable to some Rhamnaceae species but markedly lower than in *Malus domestica* and *Prunus davidiana*, suggesting lineage-specific gene losses or gains during evolution [51].

In contrast, the cpgenome (160,470 bp, 37% GC) retains the canonical quadripartite structure and gene content (113 genes, including 79 PCGs), consistent with the high conservation of chloroplast genomes across angiosperms [42]. Functional annotation confirmed the presence of 46 photosynthesis-related genes and 59 self-replication genes, reinforcing the central role of chloroplasts in light capture and autonomous genetic machinery. The identification of 17 intron-containing genes, with *ycf3* and *clpP* each containing two introns, mirrors the conserved intron distribution pattern observed in other Rhamnaceae cpgenomes [52, 53].

RSCU values measure the ratio of observed codon frequencies to those expected under uniform synonymous usage, reflecting species-specific codon preferences and underlying evolutionary pressures [54]. In both *P. hemsleyanus* organellar genomes, 30 codons showed RSCU values > 1, most of which were biased toward A or U-ending triplets. These distinct RSCU patterns suggest that both mutational bias and translational selection shape codon usage in *P. hemsleyanus* organellar genomes, in agreement with evolutionary dynamics observed in other plants [55, 56].

Repetitive elements showed striking inter-organelle divergence. The mitogenome contained significantly more SSRs (102 vs 65) and dispersed repeats (734 vs 201) than the cpgenome, which is consistent with the higher structural plasticity of plant mitogenomes [41, 57]. Mononucleotide A/T repeats dominated

both genomes, while dinucleotide and tetranucleotide repeats were preferentially retained in the mitogenome. The abundance of reverse and palindromic repeats in the mitogenome likely promotes recombination events, contributing to genome rearrangements and size variation, as proposed previously [49, 58]. The absence of complementary repeats in the mitogenome and their presence (2 copies) in the cpgenome may reflect lineage-specific repeat evolution in *P. hemsleyanus* [51].

Collectively, our comprehensive characterization demonstrates that the *P. hemsleyanus* mitogenome and cpgenome exhibit distinct evolutionary trajectories: the mitogenome is moderately sized, GC-stable, and repeat-rich, while the cpgenome is structurally conserved and gene-dense. These findings, together with our previous analyses of nuclear-organelle interactions, RNA editing, DNA transfer, and phylogeny, provide an integrated evolutionary framework for *P. hemsleyanus*. The study not only fills a knowledge gap in Rhamnaceae organellar genomics but also lays a foundation for future investigations into genetic improvement, ecological adaptation, and evolutionary diversification of this economically important species.

4.2 Characterization of RNA editing events and MTPTs in *P. hemsleyanus* mitochondrial genome

RNA editing is a crucial post-transcriptional regulatory mechanism that ensures the accurate expression of functional proteins in plant mitochondria, as it corrects genetic information encoded in the mitochondrial genome to restore evolutionarily conserved amino acids critical for protein structure and function [59–61]. In this study, we systematically predicted RNA editing sites across all PCGs in the *P. hemsleyanus* mitochondrial genome, and all identified editing events were C-to-U transitions—consistent with the canonical editing type universally observed in angiosperm mitochondria, where non-canonical editing types are extremely rare [62]. This conservation highlights the evolutionary significance of C-to-U editing in maintaining mitochondrial function across plant lineages.

The number of RNA editing sites varied substantially among mitochondrial PCGs in *P. hemsleyanus*, reflecting gene-specific functional constraints rather than uniform editing across all genes. The *nad4* gene harbored the highest number of editing sites (49), which aligns with previous studies showing that *nad* gene family members (encoding subunits of respiratory chain complex I) often exhibit high editing densities due to their critical role in mitochondrial energy metabolism [63]. Similarly, *ccmB* (35 sites), *nad7* (36 sites), *matR* (33 sites), and *nad1* (33 sites) also displayed high editing frequencies: *ccmB* is involved in cytochrome c maturation, a process essential for respiratory chain function [64], while *matR* plays a key role in intron splicing of mitochondrial genes, explaining its elevated editing requirement [65, 66]. In contrast, genes such as *rps7* and *sdh4* contained only 2–7 editing sites. Collectively, these results indicate that RNA editing in *P. hemsleyanus* mitochondria is functionally associated with gene importance, with genes involved in core respiratory processes and intron splicing requiring more extensive editing to maintain their functionality.

Inter-organellar DNA transfer, particularly MTPT, is a hallmark of plant organellar genome evolution, contributing significantly to the structural complexity and evolutionary dynamics of mitochondrial

genomes[49, 67]. We identified 17 MTPT fragments in the *P. hemsleyanus* mitogenome, with a cumulative length of 17,718 bp accounting for approximately 4.55% of the total mitogenome size—within the typical 1–10% range reported for seed plants [68]. MTPT fragment lengths ranged from 31 bp to 7,219 bp, reflecting heterogeneous insertions from both ancient degraded transfers and recent nearly intact integrations [49, 51].

Notably, the conserved functional elements within MTPTs, such as the tRNA genes *trnM-CAU*, *trnN-GUU*, *trnD-GUC*, and *trnH-GUG* present in both organellar genomes, highlight the functional significance of inter-organellar DNA transfer. Functional plastid-derived tRNAs can be transcribed in mitochondria and even replace native mitochondrial tRNA counterparts, ensuring the accurate translation of mitochondrial genes [69, 70]. The presence of these conserved tRNA genes in MTPTs suggests that chloroplast-derived sequences not only contribute to the structural complexity of the *P. hemsleyanus* mitochondrial genome but also play a functional role in maintaining mitochondrial translation machinery.

Collectively, our findings on RNA editing and inter-organellar DNA transfer in *P. hemsleyanus* are consistent with those documented across diverse angiosperm lineages, reinforcing the conserved roles of these processes in shaping mitochondrial genome evolution [49, 62]. The gene-specific RNA editing patterns highlight the functional association between editing frequency and mitochondrial gene importance, while the extensive MTPTs underscore the dynamic nature of inter-organellar crosstalk. These results not only provide new insights into the evolutionary mechanisms of the *P. hemsleyanus* mitochondrial genome but also lay a foundation for future studies on the functional implications of RNA editing and MTPTs in this economically and ecologically important Rhamnaceae species.

4.3 Comparative synteny, evolutionary selection and phylogenetic relationships in *P. hemsleyanus* mitochondrial genome

Comparative collinearity analysis is a powerful tool for evaluating mitochondrial genome assembly quality and deciphering structural evolutionary dynamics, as it reveals sequence homology, syntenic conservation, and genomic rearrangements among related species [8, 71].

In this study, collinearity analysis between *P. hemsleyanus* and three closely related Rhamnaceae species (*Frangula alnus*, *Ziziphus jujuba* and *Ziziphus mauritiana*) revealed extensive sequence homology across the four genomes, with shared syntenic blocks confirming the high assembly quality of the *P. hemsleyanus* mitochondrial genome. The presence of conserved syntenic blocks alongside extensive rearrangements suggests a balance between evolutionary conservation (to maintain core functions) and structural plasticity (to drive adaptive evolution), a pattern that has been documented in other angiosperm lineages [49, 72].

Analysis of Ka/Ks ratios revealed heterogeneous selective pressures acting on mitochondrial PCGs in *P. hemsleyanus*, reflecting functional differences and evolutionary constraints among gene families. Most mitochondrial genes exhibited Ka/Ks values below 1, indicating strong purifying selection—consistent

with the conservation of core mitochondrial functions essential for plant growth and development [73, 74]. In contrast, several genes displayed signals of relaxed or positive selection: the *atp8* gene exhibited the highest Ka/Ks ratio (> 2), suggesting strong positive selection, which may be associated with adaptive changes in ATP synthase function to cope with specific environmental conditions [75, 76].

Other genes, including *ccmFc*, *matR*, *nad1*, *rpl5*, and *rps4*, also showed elevated Ka/Ks values (> 1), consistent with positive or relaxed selective pressure. These genes are involved in cytochrome c maturation (*ccmFc*), intron splicing (*matR*), respiratory chain function (*nad1*), and ribosomal assembly (*rpl5*, *rps4*), suggesting that adaptive evolution in these processes may contribute to the ecological adaptation of *P. hemsleyanus* [76, 77]. Notably, genes involved in core respiratory functions (e.g., *atp1*, *atp4*, *cox1*, *cox2*) generally displayed Ka/Ks values below 0.5, indicating extremely strong purifying selection to maintain their functional integrity—consistent with their indispensable role in mitochondrial energy metabolism [8, 78].

Phylogenetic analysis based on concatenated core mitochondrial PCGs from 21 representative species across 6 families yielded a ML tree with robust topology, clearly resolving the phylogenetic position of *P. hemsleyanus* within Rhamnaceae. The tree strongly supports the monophyly of the Rhamnaceae family, with *P. hemsleyanus* forming a well-supported clade with *Frangula alnus*, *Ziziphus jujuba*, and *Ziziphus mauritiana*—confirming their close evolutionary relationship and validating the taxonomic placement of *P. hemsleyanus* within Rhamnaceae. This result aligns with established angiosperm taxonomy and previous mitochondrial-based phylogenetic studies [79], as well as recent plastome-based analyses of Rhamnaceae that have revised the family's phylogenetic framework based on chloroplast sequences [1, 80]. All species clustered into their respective families (Moraceae, Elaeagnaceae, Rosaceae, Fabaceae, Gramineae) with high bootstrap support, further confirming the reliability of the phylogenetic tree and the utility of core mitochondrial PCGs for resolving inter-familial and intra-familial relationships in angiosperms [74].

Collectively, these analyses validate the assembly integrity and taxonomic placement of *P. hemsleyanus*, while revealing the complex evolutionary dynamics shaping its mitochondrial genome. The multi-chromosomal structure and widespread genomic rearrangements of the *P. hemsleyanus* mitochondrial genome distinguish it from closely related Rhamnaceae species, reflecting lineage-specific structural evolution. Heterogeneous selective pressures, with strong purifying selection on core respiratory genes and positive/relaxed selection on specific functional genes, underscore the adaptive potential of mitochondrial genes during *P. hemsleyanus* evolution. The well-supported phylogenetic placement of *P. hemsleyanus* within Rhamnaceae provides a robust evolutionary framework for future studies on the diversification and adaptation of this economically and ecologically important species. These findings, together with our previous analyses of RNA editing and inter-organellar DNA transfer, offer comprehensive insights into the evolutionary mechanisms governing the *P. hemsleyanus* mitochondrial genome.

4.4 PPI network reveals key regulatory modules of nuclear-mitochondrial interaction in *P. hemsleyanus*

PPI network analysis offers a systems-level understanding of the functional coordination between nuclear and organellar genomes, which is essential for deciphering the molecular mechanisms underlying organellar physiology and plant growth [81–83]. Subcellular localization prediction using a consensus strategy across multiple independent platforms has become a gold standard for identifying high-confidence organelle-targeted proteins, effectively minimizing false-positive predictions and ensuring the reliability of downstream PPI network construction. In this study, we employed three widely used bioinformatic tools (TargetP, WoLF PSORT, and DeepLoc) to prioritize 72 high-confidence nuclear-encoded DEGs targeted to chloroplast (50) and mitochondrion (22), providing a robust foundation for investigating the regulatory crosstalk between the nucleus and organelles in *P. hemsleyanus*.

The chloroplast-targeted PPI network revealed a highly interconnected core module dominated by key components of the photosynthetic apparatus and carbon fixation machinery, including subunits of photosystem I/II, the cytochrome b_6f complex, ATP synthase, and chloroplast ribosomal proteins—consistent with the extensive physical and functional interactions required for efficient light capture, electron transfer, and energy conversion [84–86]. Among the key nuclear-encoded plastid-targeted hub proteins, RBCS-1A and RBCS-3B, as small subunits of Rubisco (ribulose bisphosphate carboxylase/oxygenase), formed a central sub-network with Calvin cycle enzymes (GAPA1, FBA2), underscoring their pivotal role as nuclear-plastid connectors that link nuclear transcriptional regulation to carbon fixation efficiency—a critical process for plant growth and biomass accumulation [87–89]. The light-harvesting complex proteins (LHCA1/2/3/4, LHCB5) formed a tightly interconnected module with photosystem core components, which is consistent with their well-documented function in maximizing light absorption and protecting photosystems from photodamage [90]. Additionally, chaperonin subunits CPN60A1 and CPN60B1 interacted with a broad range of chloroplast proteins, highlighting their essential role in protein folding and the assembly of photosynthetic complexes [91, 92]. FD1 (Ferredoxin 1) emerged as another major hub, with extensive connections to photosynthetic electron transport chain components, implicating its central role in mediating electron flow, redox regulation, and the coordination of cyclic electron transport with photoprotection [93, 94]. Collectively, these findings indicate that the chloroplast-targeted PPI network integrates photosynthesis, carbon fixation, protein homeostasis, and stress responses, reflecting the intricate regulatory mechanisms by which nuclear-encoded proteins modulate chloroplast function in *P. hemsleyanus*.

Parallel to the chloroplast network, the mitochondrion-targeted PPI network exhibited a highly interconnected core module composed of mitochondrial respiratory chain subunits (e.g., COX1/2/3, NAD4/7/9, SDH4), ribosomal proteins (e.g., RPS7/10/12, RPL16), and metabolic regulators—reflecting the functional integration between energy metabolism, protein translation, and cellular redox balance [95, 96]. Key nuclear-encoded regulators in this network play distinct roles in mediating mitochondrial function: T20K12.260 interacted with multiple respiratory chain and ribosomal components, suggesting

its potential involvement in mitochondrial biogenesis and the coordination of energy metabolism with protein synthesis [97]; SHM1 (Serine hydroxymethyltransferase 1) connected to core respiratory and ribosomal proteins, indicating its role in one-carbon metabolism and the maintenance of mitochondrial redox balance—an essential process for plant stress tolerance and energy production [98]. GDH2 (Glutamate dehydrogenase 2) and FDH1 (Formate dehydrogenase 1) are associated with the central respiratory network, linking amino acid and one-carbon metabolism to mitochondrial energy production, which aligns with previous studies highlighting their role in integrating carbon and nitrogen metabolism under environmental stress [99, 100]. Furthermore, PURU2 (formyltetrahydrofolate deformylase 2) participates in photorespiratory one-carbon metabolism, while LPD1 (dihydrolipoamide dehydrogenase) is involved in photorespiratory metabolism and mitochondrial redox homeostasis. Notably, the interaction observed in this study between the predominantly plastid-localized AtLPD1 and mitochondrial respiratory subunits is unexpected, implying a previously unrecognized function of LPD1 in inter-organellar redox crosstalk, or the possibility of its low-abundance dual targeting to mitochondrion [101]. NDPK3 (nucleoside diphosphate kinase 3) further modulates nucleotide metabolism and mitochondrial redox homeostasis[102]. Collectively, these findings highlight the multilayered regulatory functions of nuclear-encoded proteins in sustaining mitochondrial performance.

Notably, the distinct topological features of the two PPI networks reflect the specialized functional roles of chloroplast and mitochondrion in *P. hemsleyanus*: the chloroplast network is centered on photosynthetic and carbon fixation processes, while the mitochondrial network is dominated by energy metabolism and metabolic integration—consistent with the core physiological functions of these two organelles (Jarvis and López-Juez, 2013; Huang et al., 2019) [40, 103]. The hub proteins identified in this study (e.g., RBCS-1A, FD1, CPN60A1 in chloroplast; T20K12.260, SHM1, GDH2 in mitochondria) represent promising candidates for future functional studies, as they likely serve as key regulators of organellar function and nuclear-organelle crosstalk. The identification of species-specific hub proteins in *P. hemsleyanus* suggests a potential molecular basis for its unique ecological adaptations and economic traits.

Collectively, our PPI network analyses reveal the intricate functional coordination between nuclear-encoded organellar proteins and their organellar targets in *P. hemsleyanus*. The chloroplast-targeted network integrates photosynthesis, carbon fixation, and stress responses, while the mitochondrion-targeted network highlights the centrality of the respiratory chain and its connections to amino acid, nucleotide, and one-carbon metabolism. These findings not only provide a molecular framework for understanding nuclear-organelle crosstalk in *P. hemsleyanus* but also lay the foundation for future studies on the genetic improvement of this economically and ecologically important Rhamnaceae species.

5. Conclusion

To sum up, this research presents the high-quality assembly, along with comparative mitogenomic and chloroplast genomic analyses, of *P. hemsleyanus*, thereby establishing a critical genomic resource for the

Rhamnaceae family. Our multi-faceted comparative investigation uncovers the key characteristics of the organelle genome. These results not only shed light on the evolutionary patterns of organellar genomes during the domestication process but also offer a high-standard reference for subsequent genomics research and molecular breeding endeavors. A major conceptual breakthrough of this work is the integration of transcriptomic data to construct the nuclear-organellar PPI network in *P. hemsleyanus*. This network-based approach goes beyond conventional organelle descriptions by revealing regulatory connections across different cellular compartments. We identified some genes as core hub genes that link nuclear signaling pathways with organellar PPI. Taken together, this study establishes a novel framework for plant mitogenomic research—shifting from descriptive characterization to the inference of functional networks. The genomic resources, PPI network, and candidate genes reported in this study provide a robust foundation for future research on organelle genome evolution, nucleo-mitochondrial interactions, and molecular breeding of Rhamnaceae species.

Declarations

Ethics approval and consent to participate

Not applicable.

Consent for publication

Not applicable.

Declaration of competing interest

The authors declare no competing interests.

Funding

This work was supported by the research startup fund for high-level talents (grant No. DT2600000516).

CRediT authorship contribution statement

Yanzhao Zhang and Haoxing Li conceived, designed, and supervised the entire research project. Botao Ye, Rong Chen, Xuhui Li, and Shiting Yang were responsible for plotting the figures included in the manuscript. Botao Ye drafted the initial version of the manuscript, and all authors participated in the writing, revision, and editing of the final manuscript.

Data Availability

The organellar genome assemblies generated in this study have been deposited in the Figshare repository under the DOI https://doi.org/10.6084/m9.figshare.32338785. For publicly available reference datasets, PacBio HiFi sequencing data of P. hemsleyanus were obtained from the Genome Sequence Archive (GSA) under accession CRR1721099 (https://ngdc.cncb.ac.cn/gsa/browse/CRA024427/CRR1721099), and publicly available RNA-seq data from roots, stems, and leaves of P. hemsleyanus were retrieved from the China National Center for Bioinformation (CNCB) under BioProject PRJCA038194 (https://ngdc.cncb.ac.cn/bioproject/browse/PRJCA038194).

References

1. Zhang S, Guo J, Lin D, Shen J, Zhang Z, Yang Y, Lan Y, Li J, Zhao J, Li Y *et al*: **Haplotype-resolved t2t genome of *paliurus hemsleyanus* provides insights into rhamnaceae evolution and genome biology**. *Communications biology* 2025, **8**(1):1744.
2. Shoei-Sheng L, Shew-Neu S, Liu KCS: **Triterpenes from *Paliurus hemsleyanus***. *Phytochemistry* 1997, **46**(3):549-554.
3. Yang M, Han L, Zhang S, Dai L, Li B, Han S, Zhao J, Liu P, Zhao Z, Liu M: **Insights into the evolution and spatial chromosome architecture of jujube from an updated gapless genome assembly**. *Plant communications* 2023, **4**(6):100662.
4. Xu Y, Wang C, Kong D, Cao M, Zhang Q, Tahir M, Yang Y, Yang S, Bo W, Pang X: **Identification of high tolerance to jujube witches' broom in Indian jujube (*Ziziphus mauritiana* Lam.) and mining differentially expressed genes related to the tolerance through transcriptome analysis**. *Plants* 2023, **12**(11):2082.
5. Gabaldón T: **Origin and early evolution of the eukaryotic cell**. *Annu Rev Microbiol* 2021, **75**:631-647.
6. Sloan DB, Warren JM, Williams AM, Wu Z, Abdel-Ghany SE, Chicco AJ, Havird JC: **Cytonuclear integration and co-evolution**. *Nature Reviews Genetics* 2018, **19**(10):635-648.
7. Wu Z-Q, Liao X-Z, Zhang X-N, Tembrock LR, Broz A: **Genomic architectural variation of plant mitochondria-A review of multichromosomal structuring**. *Journal of Systematics and Evolution* 2022, **60**(1):160-168.
8. Kozik A, Rowan BA, Lavelle D, Berke L, Schranz ME, Michelmore RW, Christensen AC: **The alternative reality of plant mitochondrial DNA: One ring does not rule them all**. *PLoS Genet* 2019, **15**(8):e1008373.
9. Gualberto JM, Mileshina D, Wallet C, Niazi AK, Weber-Lotfi F, Dietrich A: **The plant mitochondrial genome: dynamics and maintenance**. *Biochimie* 2014, **100**:107-120.
10. Daniell H, Lin C-S, Yu M, Chang W-J: **Chloroplast genomes: diversity, evolution, and applications in genetic engineering**. *Genome Biology* 2016, **17**(1):134.
11. Wu Y, Zeng J, Zhang F, Zhu Z, Qi T, Zheng Z, Lloyd-Jones LR, Marioni RE, Martin NG, Montgomery GW *et al*: **Integrative analysis of omics summary data reveals putative mechanisms underlying complex traits**. *Nature Communications* 2018, **9**(1):918.

12. Zhou C, Brown M, Blaxter M, McCarthy SA, Durbin R, Darwin Tree of Life Project C: **Oatk: a de novo assembly tool for complex plant organelle genomes**. *Genome Biology* 2025, **26**(1):235.
13. Bi C, Shen F, Han F, Qu Y, Hou J, Xu K, Xu LA, He W, Wu Z, Yin T: **PMAT: an efficient plant mitogenome assembly toolkit using low-coverage HiFi sequencing data**. *Hortic Res* 2024, **11**(3):uhae023.
14. Tillich M, Lehwark P, Pellizzer T, Ulbricht-Jones ES, Fischer A, Bock R, Greiner S: **GeSeq - versatile and accurate annotation of organelle genomes**. *Nucleic Acids Res* 2017, **45**(W1):W6-W11.
15. Kearse M, Moir R, Wilson A, Stones-Havas S, Cheung M, Sturrock S, Buxton S, Cooper A, Markowitz S, Duran C *et al*: **Geneious Basic: an integrated and extendable desktop software platform for the organization and analysis of sequence data**. *Bioinformatics (Oxford, England)* 2012, **28**(12):1647-1649.
16. Greiner S, Lehwark P, Bock R: **OrganellarGenomeDRAW (OGDRAW) version 1.3.1: expanded toolkit for the graphical visualization of organellar genomes**. *Nucleic Acids Research* 2019, **47**(W1):W59-W64.
17. Fitch WM: **The relation between frequencies of amino acids and ordered trinucleotides**. *J Mol Biol* 1966, **16**(1):1-8.
18. Beier S, Thiel T, Münch T, Scholz U, Mascher M: **MISA-web: a web server for microsatellite prediction**. *Bioinformatics* 2017, **33**(16):2583-2585.
19. Benson G: **Tandem repeats finder: a program to analyze DNA sequences**. *Nucleic Acids Res* 1999, **27**(2):573-580.
20. Kurtz S: **The Vmatch large scale sequence analysis software-A Manual**. *Center for Bioinformatics* 2010, **170**(24):391–392.
21. Edera AA, Small I, Milone DH, Sanchez-Puerta MV: **Deepred-Mt: Deep representation learning for predicting C-to-U RNA editing in plant mitochondria**. *Comput Biol Med* 2021, **136**:104682.
22. Camacho C, Coulouris G, Avagyan V, Ma N, Papadopoulos J, Bealer K, Madden TL: **BLAST+: architecture and applications**. *BMC Bioinformatics* 2009, **10**(1):421.
23. Zhang H, Meltzer P, Davis S: **RCircos: an R package for Circos 2D track plots**. *BMC Bioinformatics* 2013, **14**:244.
24. Darling ACE, Mau B, Blattner FR, Perna NT: **Mauve: multiple alignment of conserved genomic sequence with rearrangements**. *Genome Res* 2004, **14**(7):1394-1403.
25. Katoh K, Standley DM: **MAFFT multiple sequence alignment software version 7: improvements in performance and usability**. *Mol Biol Evol* 2013, **30**(4):772-780.
26. Capella-Gutiérrez S, Silla-Martínez JM, Gabaldón T: **trimAl: a tool for automated alignment trimming in large-scale phylogenetic analyses**. *Bioinformatics* 2009, **25**(15):1972-1973.
27. Zhang Z: **KaKs_calculator 3.0: calculating selective pressure on coding and non-coding sequences**. *Genomics, proteomics & bioinformatics* 2022, **20**(3):536-540.

28. Stamatakis A: **RAxML version 8: a tool for phylogenetic analysis and post-analysis of large phylogenies**. *Bioinformatics* 2014, **30**(9):1312-1313.
29. Xie J, Chen Y, Cai G, Cai R, Hu Z, Wang H: **Tree Visualization By One Table (tvBOT): a web application for visualizing, modifying and annotating phylogenetic trees**. *Nucleic Acids Research* 2023, **51**(W1):W587-W592.
30. Chen S, Zhou Y, Chen Y, Gu J: **fastp: an ultra-fast all-in-one FASTQ preprocessor**. *Bioinformatics* 2018, **34**(17):i884-i890.
31. Kim D, Paggi JM, Park C, Bennett C, Salzberg SL: **Graph-based genome alignment and genotyping with HISAT2 and HISAT-genotype**. *Nature Biotechnology* 2019, **37**(8):907-915.
32. Liao Y, Smyth GK, Shi W: **FeatureCounts: an efficient general purpose program for assigning sequence reads to genomic features**. *Bioinformatics* 2014, **30**(7):923-930.
33. Robinson MD, McCarthy DJ, Smyth GK: **EdgeR: a Bioconductor package for differential expression analysis of digital gene expression data**. *Bioinformatics* 2010, **26**(1):139-140.
34. Wu T, Hu E, Xu S, Chen M, Guo P, Dai Z, Feng T, Zhou L, Tang W, Zhan L *et al*: **clusterProfiler 4.0: A universal enrichment tool for interpreting omics data**. *Innovation* 2021, **2**(3):100141.
35. Almagro Armenteros JJ, Salvatore M, Emanuelsson O, Winther O, von Heijne G, Elofsson A, Nielsen H: **Detecting sequence signals in targeting peptides using deep learning**. *Life science alliance* 2019, **2**(5):e201900429.
36. Horton P, Park KJ, Obayashi T, Fujita N, Harada H, Adams-Collier CJ, Nakai K: **WoLF PSORT: protein localization predictor**. *Nucleic Acids Res* 2007, **35**(Web Server issue):W585-W587.
37. Thumuluri V, Almagro Armenteros JJ, Johansen AR, Nielsen H, Winther O: **DeepLoc 2.0: multi-label subcellular localization prediction using protein language models**. *Nucleic Acids Res* 2022, **50**(W1):W228-W234.
38. Szklarczyk D, Kirsch R, Koutrouli M, Nastou K, Mehryary F, Hachilif R, Gable AL, Fang T, Doncheva NT, Pyysalo S *et al*: **The STRING database in 2023: protein-protein association networks and functional enrichment analyses for any sequenced genome of interest**. *Nucleic Acids Res* 2023, **51**(D1):D638-D646.
39. Shannon P, Markiel A, Ozier O, Baliga NS, Wang JT, Ramage D, Amin N, Schwikowski B, Ideker T: **Cytoscape: a software environment for integrated models of biomolecular interaction networks**. *Genome Res* 2003, **13**(11):2498-2504.
40. Jarvis P, López-Juez E: **Biogenesis and homeostasis of chloroplasts and other plastids**. *Nature reviews Molecular cell biology* 2013, **14**(12):787-802.
41. Sloan DB: **One ring to rule them all? Genome sequencing provides new insights into the 'master circle' model of plant mitochondrial DNA structure**. *The New phytologist* 2013, **200**(4):978-985.
42. Jansen RK, Cai Z, Raubeson LA, Daniell H, Depamphilis CW, Leebens-Mack J, Müller KF, Guisinger-Bellian M, Haberle RC, Hansen AK *et al*: **Analysis of 81 genes from 64 plastid genomes resolves relationships in angiosperms and identifies genome-scale evolutionary patterns**. *Proc Natl Acad Sci U S A* 2007, **104**(49):19369-19374.

43. Fang B, Li J, Zhao Q, Liang Y, Yu J: **Assembly of the complete mitochondrial genome of Chinese plum (*Prunus salicina*): characterization of genome recombination and RNA editing sites**. *Genes* 2021, **12**(12):1970.
44. Wang X, Cheng F, Rohlsen D, Bi C, Wang C, Xu Y, Wei S, Ye Q, Yin T, Ye N: **Organellar genome assembly methods and comparative analysis of horticultural plants**. *Hortic Res* 2018, **5**:3.
45. Zhang Y, Guo X, Ma R, Yu M, Xu J, Shen Z: **Assembly and analysis of the complete mitochondrial genome of *Prunus davidiana* (Rosaceae)**. *Front Plant Sci* 2025, **16**:1558619.
46. Jialei L, Chu Z, Yisilam G, Wang Y, Zheng E, Li C, Su Y, Tian X: **The complete mitochondrial genomes of two apple cultivars reveal the highly conserved structure in cultivated apples**. *Cytology and Genetics* 2025, **59**(2):228-240.
47. Fan W, Liu F, Jia Q, Du H, Chen W, Ruan J, Lei J, Li DZ, Mower JP, Zhu A: **Fragaria mitogenomes evolve rapidly in structure but slowly in sequence and incur frequent multinucleotide mutations mediated by microinversions**. *The New phytologist* 2022, **236**(2):745-759.
48. Yang M, Zhang S, Li B, Yang Y, Lan Y, Luo Z, Han L, Muhammad N, Liu M: **Comprehensive analysis of the mitochondrial genome of *Ziziphus mauritiana* Lam.: Investigating sequence structure, repeat-mediated recombination, chloroplast-derived transfer, RNA editing, and evolution**. *Scientia Horticulturae* 2024, **324**:112637.
49. Sloan DB, Wu Z: **History of plastid DNA insertions reveals weak deletion and at mutation biases in angiosperm mitochondrial genomes**. *Genome biology and evolution* 2014, **6**(12):3210-3221.
50. Ma Q, Wang Y, Li S, Wen J, Zhu L, Yan K, Du Y, Ren J, Li S, Chen Z *et al*: **Assembly and comparative analysis of the first complete mitochondrial genome of *Acer truncatum* Bunge: a woody oil-tree species producing nervonic acid**. *BMC Plant Biol* 2022, **22**(1):29.
51. Gandini CL, Sanchez-Puerta MV: **Foreign plastid sequences in plant mitochondria are frequently acquired via mitochondrion-to-mitochondrion horizontal transfer**. *Sci Rep* 2017, **7**:43402.
52. Wang J, Yang S: **The complete chloroplast genome of Rhamnus crenata Siebold & Zuccarini (Rhamnaceae)**. *Mitochondrial DNA Part B, Resources* 2021, **6**(9):2489-2490.
53. Huang J, Chen R, Li X: **Comparative analysis of the complete chloroplast genome of four known Ziziphus species**. *Genes* 2017, **8**(12):340.
54. Sharp PM, Tuohy TM, Mosurski KR: **Codon usage in yeast: cluster analysis clearly differentiates highly and lowly expressed genes**. *Nucleic Acids Res* 1986, **14**(13):5125-5143.
55. Hu Q, Li Q, Mao Y, Luo Y, Deng Z, Zhang W: **Assembly and analysis of the complete mitochondrial genome of *Leonurus japonicus* (Lamiaceae)**. *Sci Rep* 2025, **15**(1):13372.
56. Du M, Zhang X, Gao J, Bi S, Hao J, Zhang L: **Analysis of codon usage bias in the mitochondrial genome of *Pleurozia purpurea***. *Hebei University of Science and Technology* 2025, **46**(1):91-99.
57. Wynn EL, Christensen AC: **Repeats of unusual size in plant mitochondrial genomes: identification, incidence and evolution**. *G3* 2019, **9**(2):549-559.

58. Jiang M, Ni Y, Li J, Liu C: **Characterisation of the complete mitochondrial genome of Taraxacum mongolicum revealed five repeat-mediated recombinations**. *Plant Cell Reports* 2023, **42**(4):775-789.
59. Covello PS, Gray MW: **RNA editing in plant mitochondria**. *Nature* 1989, **341**(6243):662-666.
60. Sun T, Bentolila S, Hanson MR: **The Unexpected Diversity of Plant Organelle RNA Editosomes**. *Trends in Plant Science* 2016, **21**(11):962-973.
61. Gualberto JM, Lamattina L, Bonnard G, Weil JH, Grienenberger JM: **RNA editing in wheat mitochondria results in the conservation of protein sequences**. *Nature* 1989, **341**(6243):660-662.
62. Edera AA, Gandini CL, Sanchez-Puerta MV: **Towards a comprehensive picture of C-to-U RNA editing sites in angiosperm mitochondria**. *Plant Mol Biol* 2018, **97**(3):215-231.
63. Shedge V, Arrieta-Montiel M, Christensen AC, Mackenzie SA: **Plant mitochondrial recombination surveillance requires unusual RecA and MutS homologs**. *Plant Cell* 2007, **19**(4):1251-1264.
64. Kühn K, Yin G, Duncan O, Law SR, Kubiszewski-Jakubiak S, Kaur P, Meyer E, Wang Y, Small CC, Giraud E *et al*: **Decreasing electron flux through the cytochrome and/or alternative respiratory pathways triggers common and distinct cellular responses dependent on growth conditions**. *Plant Physiol* 2015, **167**(1):228-250.
65. Sultan LD, Mileshina D, Grewe F, Rolle K, Abudraham S, Glodowicz P, Niazi AK, Keren I, Shevtsov S, Klipcan L *et al*: **The reverse transcriptase/RNA maturase protein MatR is required for the splicing of various group II introns in Brassicaceae mitochondria**. *Plant Cell* 2016, **28**(11):2805-2829.
66. Zang J, Zhang T, Zhang Z, Liu J, Chen H: **DEFECTIVE KERNEL 56 functions in mitochondrial RNA editing and maize seed development**. *Plant Physiol* 2024, **194**(3):1593-1610.
67. Park S, Park S: **Intrageneric structural variation in organelle genomes from the genus Dystaenia (Apiaceae): genome rearrangement and mitochondrion-to-plastid DNA transfer**. *Front Plant Sci* 2023, **14**:1283292.
68. Lloyd AH, Timmis JN: **The origin and characterization of new nuclear genes originating from a cytoplasmic organellar genome**. *Mol Biol Evol* 2011, **28**(7):2019-2028.
69. Miyata S, Nakazono M, Hirai A: **Transcription of plastid-derived tRNA genes in rice mitochondria**. *Curr Genet* 1998, **34**(3):216-220.
70. Wang D, Rousseau-Gueutin M, Timmis JN: **Plastid sequences contribute to some plant mitochondrial genes**. *Mol Biol Evol* 2012, **29**(7):1707-1711.
71. Sloan DB, Alverson AJ, Chuckalovcak JP, Wu M, McCauley DE, Palmer JD, Taylor DR: **Rapid evolution of enormous, multichromosomal genomes in flowering plant mitochondria with exceptionally high mutation rates**. *PLoS Biol* 2012, **10**(1):e1001241.
72. Zou Y, Zhu W, Hou Y, Sloan DB, Wu Z: **The evolutionary dynamics of organellar pan-genomes in *Arabidopsis thaliana***. *Genome Biology* 2025, **26**(1):240.
73. Gualberto JM, Newton KJ: **Plant mitochondrial genomes: dynamics and mechanisms of mutation**. *Annu Rev Plant Biol* 2017, **68**:225-252.

74. Lin D, Shao B, Gao Z, Li J, Li Z, Li T, Huang W, Zhong X, Xu C, Chase MW *et al*: **Phylogenomics of angiosperms based on mitochondrial genes: insights into deep node relationships**. *BMC Biol* 2025, **23**(1):45.

75. Tian Y, Wu Z, Tian C, Yang Y, Li Z: **Phylogenetic classification and genetic insights from the complete mitochondrial genome of *Medicago ruthenica***. *Frontiers in Plant Science* 2025, **16** 1648505.

76. Xiong Y, Lei X, Xiong Y, Liu Y, Dong Z, Zhao J, Yu Q, Ma X: **Factors contributing to organelle genomes size variation and the intracellular DNA transfer in Polygonaceae**. *BMC Genomics* 2024, **25**(1):994.

77. Gong Y, Luo X, Zhang T, Zhou G, Li J, Zhang B, Li P, Huang H: **Assembly and comparative analysis of the complete mitochondrial genome of white towel gourd (Luffa cylindrica)**. *Genomics* 2024, **116**(3):110859.

78. Yu X, Feng Y, Zhang J: **Characterization of the complete mitochondrial genome of wintersweet (*Chimonanthus praecox*) and comparative analysis within magnoliids**. *Life* 2024, **14**(2):182.

79. Richardson JE, Fay MF, Cronk QC, Bowman D, Chase MW: **A phylogenetic analysis of Rhamnaceae using rbcL and trnL-F plastid DNA sequences**. *Am J Bot* 2000, **87**(9):1309-1324.

80. Yang M, Zhang S-F, Li B, Lan Y-X, Yang Y-H, Liu M-J: **Comparative analysis of 326 chloroplast genomes in Chinese jujube (*Ziziphus jujuba*): Structural variations, horizontal gene transfer events, and evolutionary patterns impacting its domestication from wild jujube**. *Journal of Systematics and Evolution* 2024, **62**(6):1069-1084.

81. Forsythe ES, Sharbrough J, Havird JC, Warren JM, Sloan DB: **CyMIRA: the cytonuclear molecular interactions reference for *Arabidopsis***. *Genome biology and evolution* 2019, **11**(8):2194-2202.

82. Di Silvestre D, Jeran N, Domingo G, Vannini C, Marsoni M, Fortunato S, de Pinto MC, Tamborrino A, Negroni YL, Zottini M *et al*: **A holistic investigation of arabidopsis proteomes altered in chloroplast biogenesis and retrograde signalling identifies *Psbo* as a key regulator of chloroplast quality control**. *Plant, cell & environment* 2025, **48**(8):6373-6396.

83. McWhite CD, Papoulas O, Drew K, Cox RM, June V, Dong OX, Kwon T, Wan C, Salmi ML, Roux SJ *et al*: **A pan-plant protein complex map reveals deep conservation and novel assemblies**. *Cell* 2020, **181**(2):460-474.e414.

84. Nelson N, Ben-Shem A: **The complex architecture of oxygenic photosynthesis**. *Nature Reviews Molecular Cell Biology* 2004, **5**(12):971-982.

85. Allen JF: **Cyclic, pseudocyclic and noncyclic photophosphorylation: new links in the chain**. *Trends in Plant Science* 2003, **8**(1):15-19.

86. Barber J: **Photosystem II: the engine of life**. *Q Rev Biophys* 2003, **36**(1):71-89.

87. Spreitzer, Robert J, Salvucci, Michael E: **Rubisco: structure, regulatory interactions, and possibilities for a better enzyme**. *Annual Review of Plant Biology* 2002, **53**:449-475.

88. Khumsupan P, Kozlowska MA, Orr DJ, Andreou AI, Nakayama N, Patron N, Carmo-Silva E, McCormick AJ: **Generating and characterizing single- and multigene mutants of the Rubisco small subunit family in *Arabidopsis***. *Journal of Experimental Botany* 2020, **71**(19):5963-5975.

89. Masanori I, Honami T, Yuji S, Amane M, Hiroyuki I: ***RBCS1A* and *RBCS3B*, two major members within the *Arabidopsis* RBCS multigene family, function to yield sufficient Rubisco content for leaf photosynthetic capacity**. *Journal of Experimental Botany* 2012, **63**(5):2159-2170.
90. Niyogi KK, Truong TB: **Evolution of flexible non-photochemical quenching mechanisms that regulate light harvesting in oxygenic photosynthesis**. *Curr Opin Plant Biol* 2013, **16**(3):307-314.
91. Hemmingsen SM, Woolford C, van der Vies SM, Tilly K, Dennis DT, Georgopoulos CP, Hendrix RW, Ellis RJ: **Homologous plant and bacterial proteins chaperone oligomeric protein assembly**. *Nature* 1988, **333**(6171):330-334.
92. Ries F, Weil HL, Herkt C, Mühlhaus T, Sommer F, Schroda M, Willmund F: **Competition co-immunoprecipitation reveals the interactors of the chloroplast CPN60 chaperonin machinery**. *Plant, cell & environment* 2023, **46**(11):3371-3391.
93. Hanke G, Mulo P: **Plant type ferredoxins and ferredoxin-dependent metabolism**. *Plant, cell & environment* 2013, **36**(6):1071-1084.
94. Yamori W, Shikanai T: **Physiological functions of cyclic electron transport around photosystem i in sustaining photosynthesis and plant growth**. *Annu Rev Plant Biol* 2016, **67**:81-106.
95. Cogliati S, Lorenzi I, Rigoni G, Caicci F, Soriano ME: **Regulation of mitochondrial electron transport chain assembly**. *J Mol Biol* 2018, **430**(24):4849-4873.
96. Priesnitz C, Becker T: **Pathways to balance mitochondrial translation and protein import**. *Genes Dev* 2018, **32**(19-20):1285-1296.
97. Zhang Y, Jaime SM, Bulut M, Graf A, Fernie AR: **The conditional mitochondrial protein complexome in the *Arabidopsis thaliana* root and shoot**. *Plant communications* 2023, **4**(5):100635.
98. Douce R, Neuburger M: **The uniqueness of plant mitochondria**. *Annual Review of Plant Biology* 1989, **40**:371-414.
99. Miyashita Y, Good AG: **NAD(H)-dependent glutamate dehydrogenase is essential for the survival of Arabidopsis thaliana during dark-induced carbon starvation**. *Journal of Experimental Botany* 2008, **59**(3):667-680.
100. Roell MS, Kuhnert F, Westhoff P, Saeheng S, Roje S, Weber APM: **Mitochondrial formate dehydrogenase links mitochondrial and cytosolic one carbon metabolism via a one-carbon shunt**. *Plant Physiol* 2026, **200**(1):kiaf623.
101. Timm S, Wittmiß M, Gamlien S, Ewald R, Florian A, Frank M, Wirtz M, Hell R, Fernie AR, Bauwe H: **Mitochondrial dihydrolipoyl dehydrogenase activity shapes photosynthesis and photorespiration of *Arabidopsis thaliana***. *The Plant Cell* 2015, **27**(7):1968-1984.
102. Jardim-Messeder D, de Souza-Vieira Y, Felix-Cordeiro T, Corrêa RL, Sachetto-Martins G: **Nucleoside diphosphate kinase family: evolutionary analysis and protective role in mitochondrial ROS production**. *Plants* 2026, **15**(8):1156.
103. Huang S, Van Aken O, Schwarzländer M, Belt K, Millar AH: **The roles of mitochondrial reactive oxygen species in cellular signaling and stress response in plants**. *Plant Physiology* 2016, **171**(3):1551-1559.

Figures

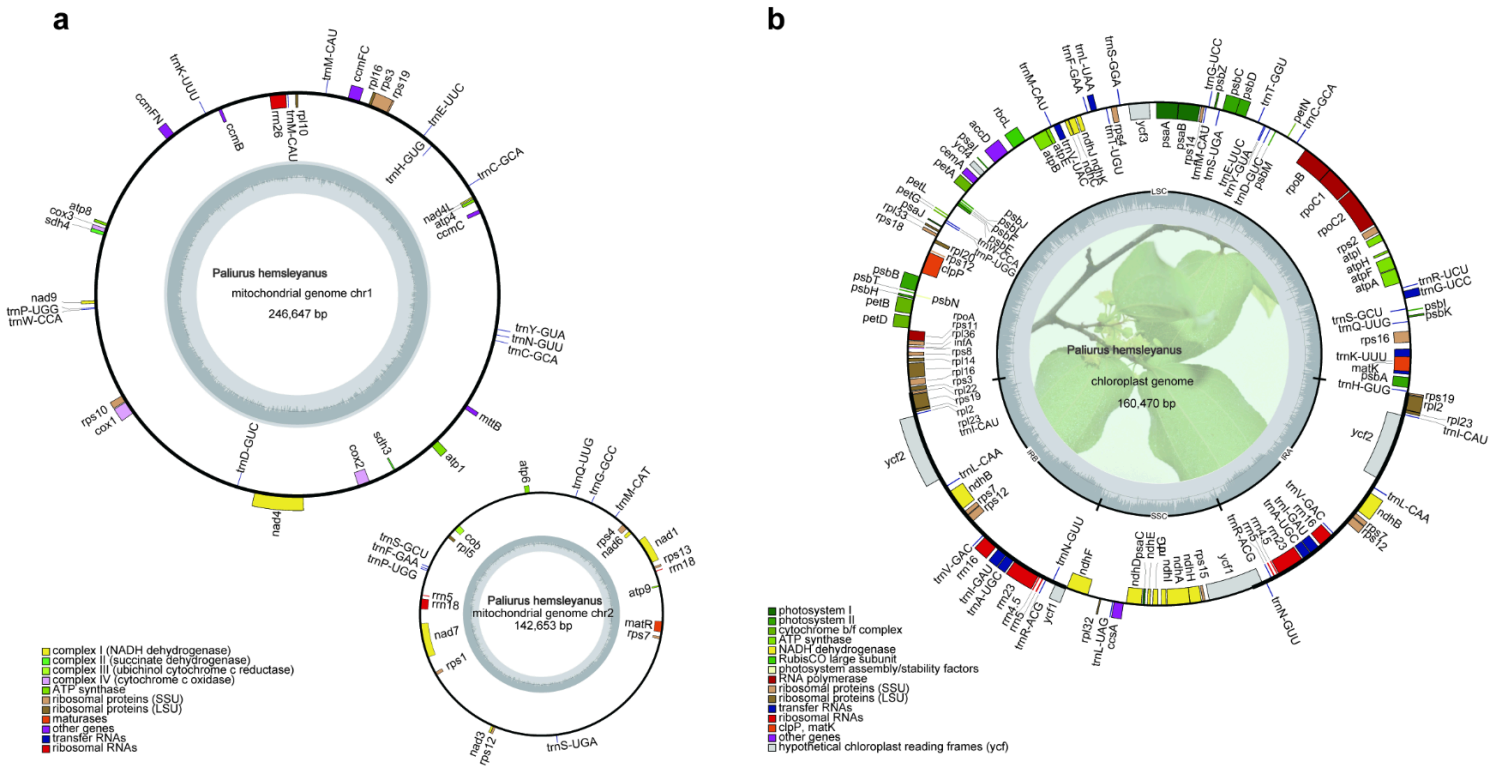


Figure 1

The organelle genomes map of *P. hemsleyanus*. (a) Genomic circular map of the *P. hemsleyanus* mitochondrion. (b) Circular visualization of the *P. hemsleyanus* chloroplast genome.

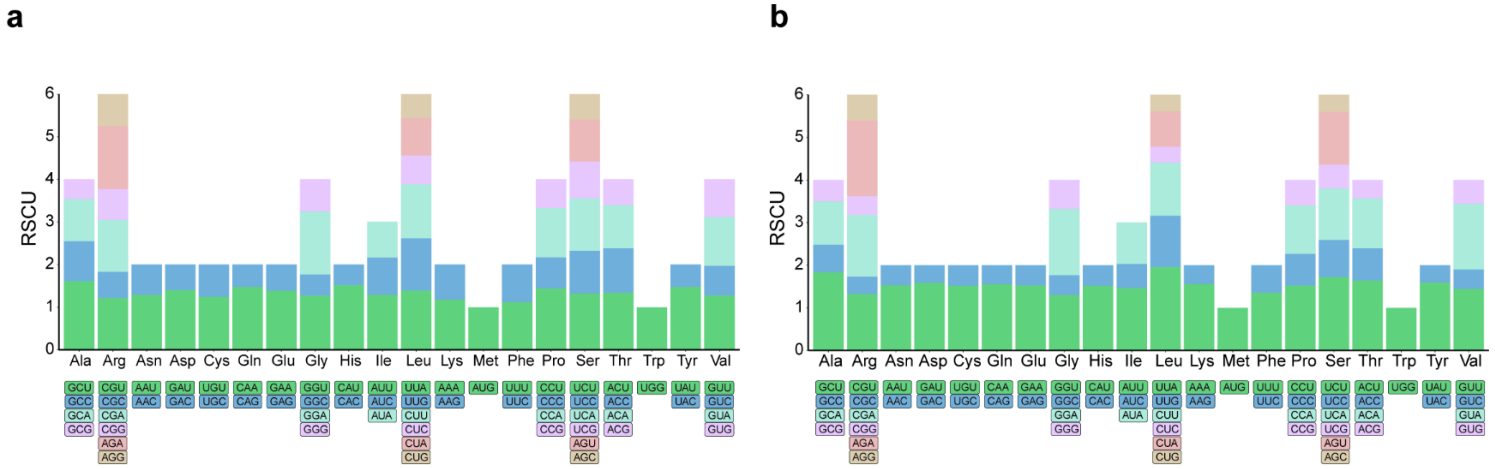


Figure 2

Summary of codon usage bias across PCGs in the organelle genomes of *P. hemsleyanus*. (a) RSCU profiles for the mitochondrial genome. (b) RSCU distribution in the chloroplast genome.

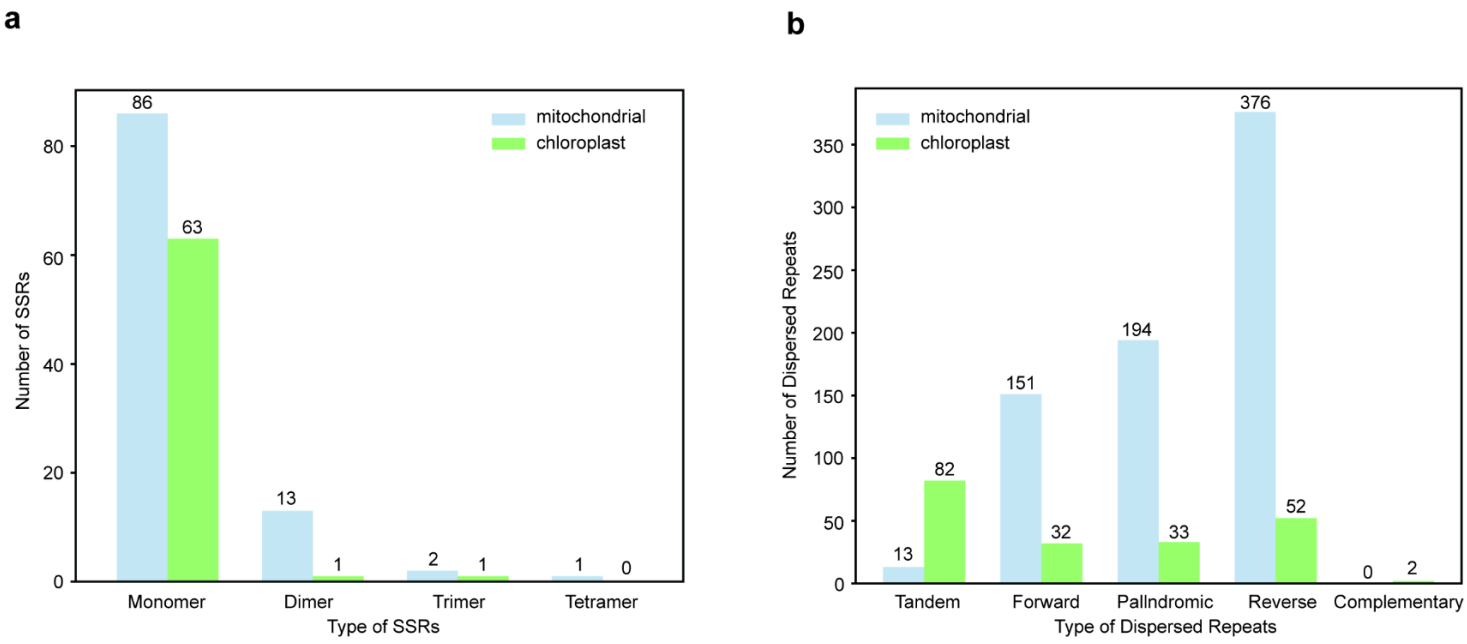


Figure 3

Comparative analysis of repeat elements between the mitochondrial and chloroplast genomes of *P. hemsleyanus*. (a) Composition of SSRs. (b) Content and distribution of DRs.

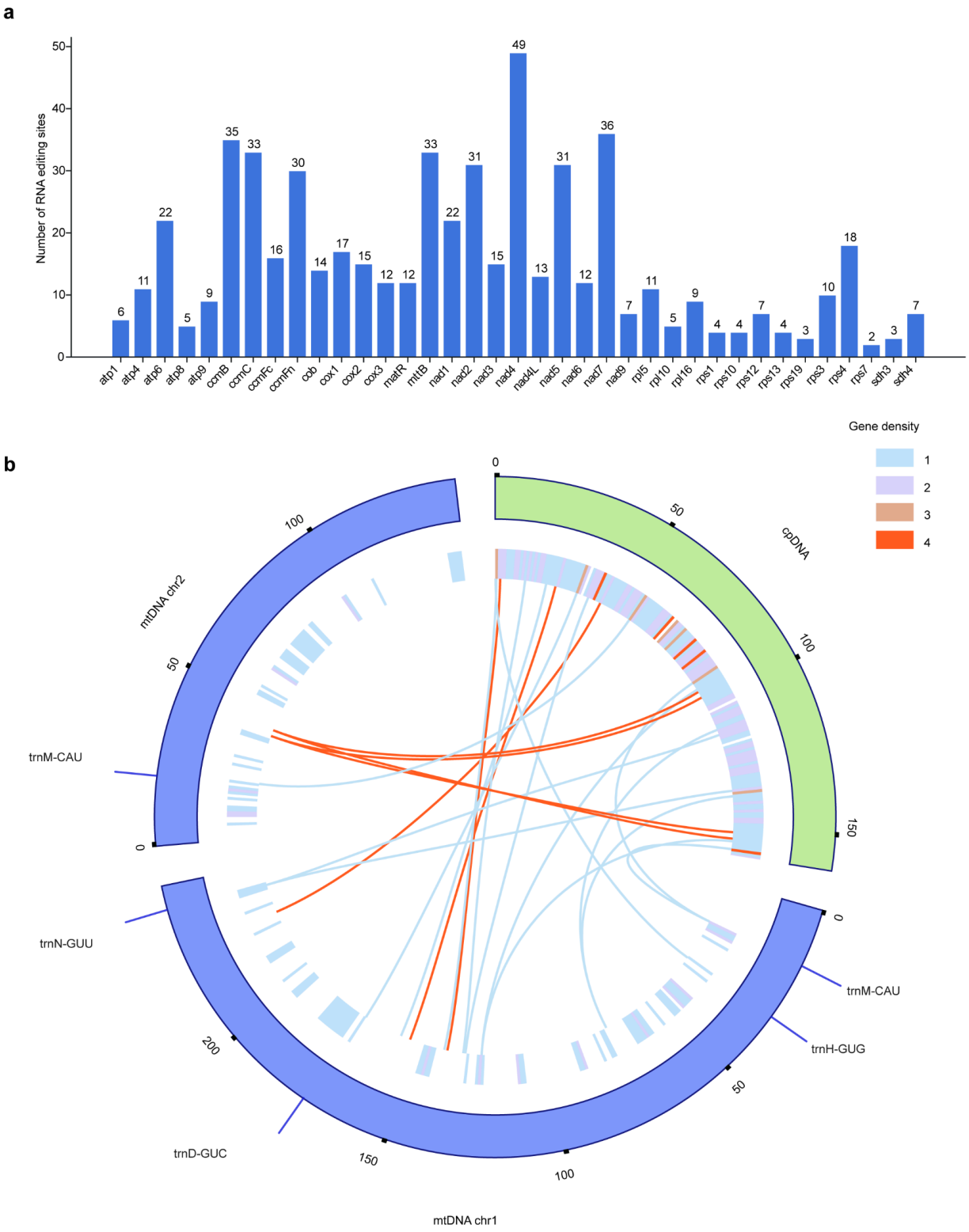


Figure 4

RNA editing site prediction and MTPT analysis of *P. hemsleyanus*. (a) Predicted RNA editing sites. (b) Genomic features of MTPTs identified in *P. hemsleyanus*.

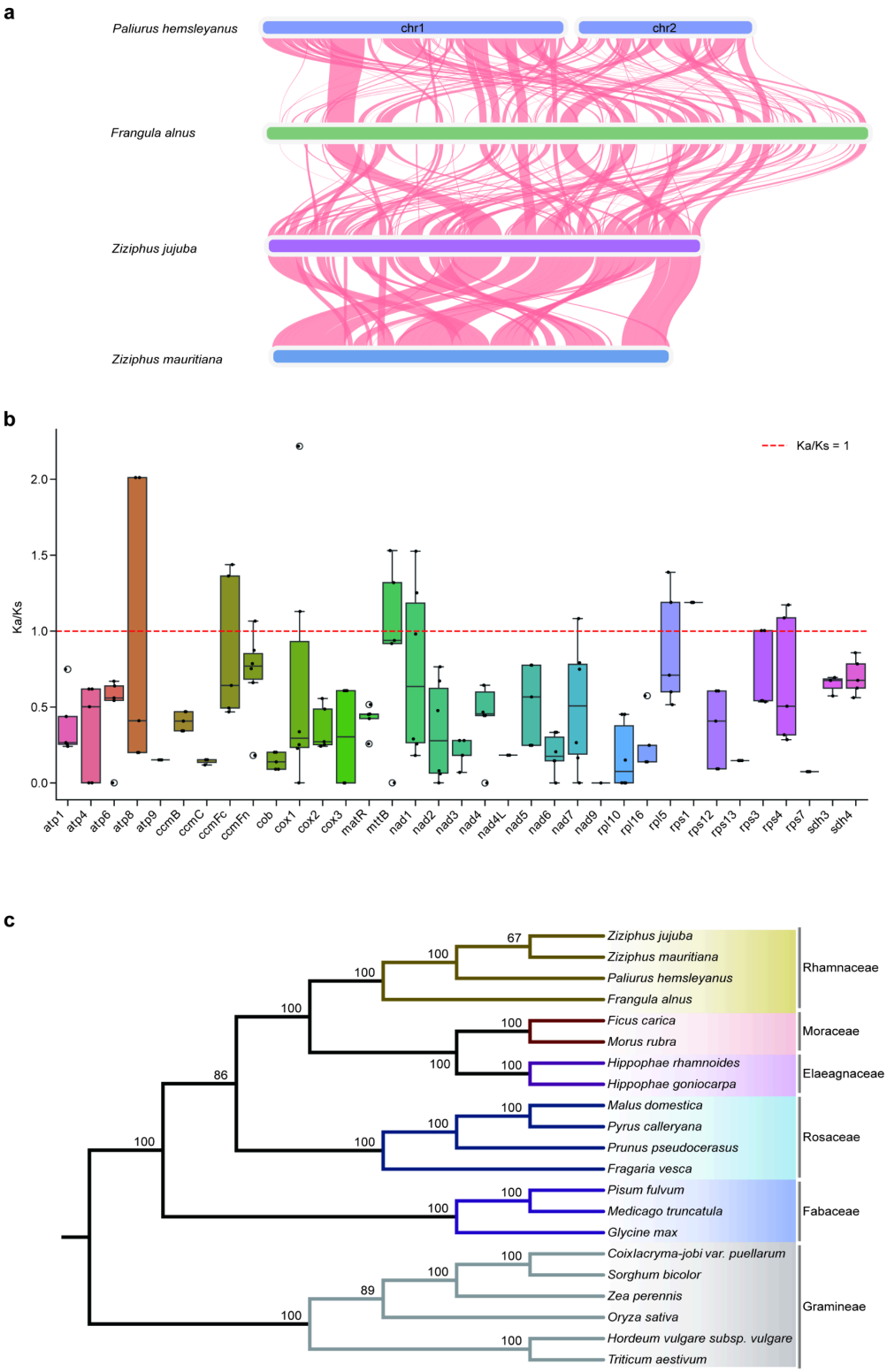


Figure 5

Comparative mitogenomic analyses and evolutionary selection pressure in *P. hemsleyanus*. (a) Synteny collinearity among the mitogenomes of four Rhamnaceae species. (b) Evolutionary selection pressure of mitochondrial genes, as indicated by Ka/Ks ratios. (c) Phylogenetic relationships inferred from 21 plant mitogenomes.

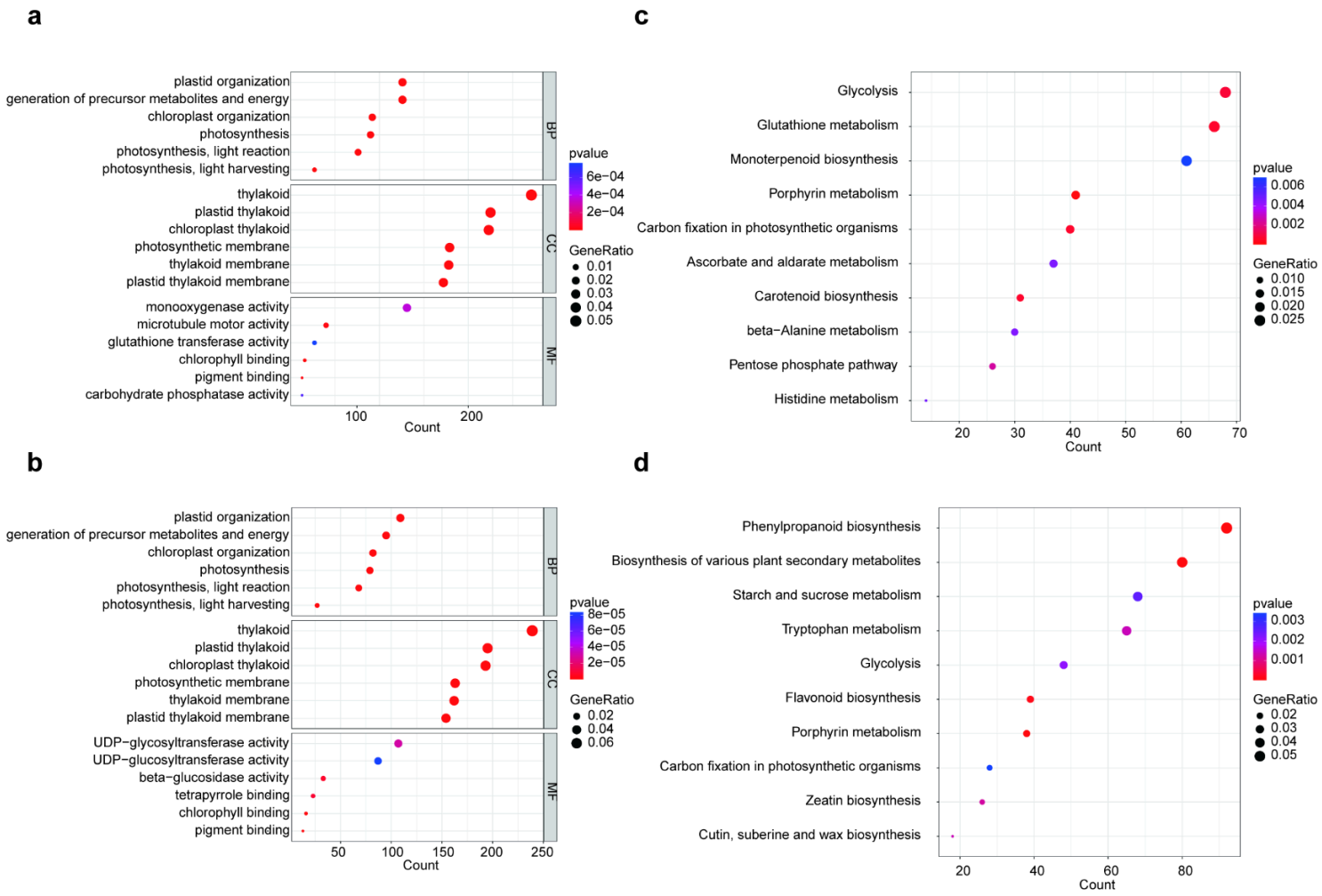


Figure 6

Transcriptomic divergence and functional enrichment profiling of DEGs in *P. hemsleyanus*. (a) Top enriched GO terms for DEGs in the root vs leaf comparison. (b) GO enrichment landscape of DEGs from the stem vs leaf contrast. (c) KEGG pathway enrichment of root-leaf DEGs. (d) KEGG pathway distribution of stem-leaf DEGs.

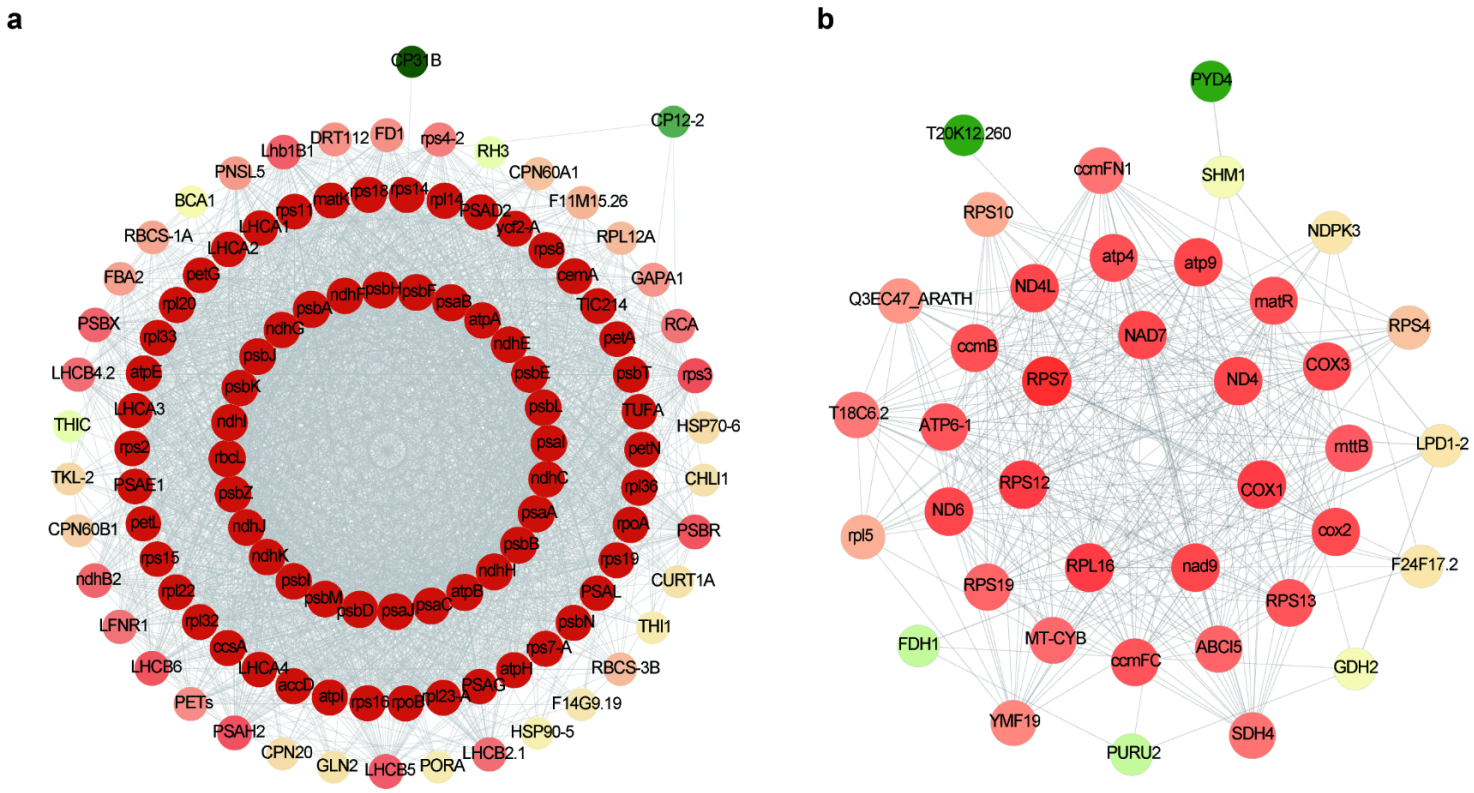


Figure 7

Organelle-targeted DEG expression profiles and their PPI landscapes in *P. hemsleyanus*. (a) Interaction network connecting nuclear DEGs to chloroplast-encoded proteins. (b) Functional characterization of the PPI network formed by nuclear DEGs and mitochondrial gene products.

Supplementary Files

This is a list of supplementary files associated with this preprint. Click to download.

- SupplementaryTables4.xlsx